ELSEVIER

Thermochimica Acta 273 (1996) 119–133

thermochimica acta

Influence of precipitation chemistry and ball-milling on the thermal behavior of zirconium hydroxide

G. Štefanić*, S. Musić, A. Sekulić

Ruđer Bošković Institute, P.O. Box 1016, 10001 Zagreb, Croatia

Received 3 April 1995; accepted 17 July 1995

Abstract

Zirconium hydroxide precipitates, obtained by rapid precipitation at pH 2.5, 7.5, and 10.5, were ball-milled for up to 60 h and then heated inside a differential scanning calorimeter (DSC) at temperatures of up to 600 °C. Crystal phases produced after heating were analyzed by FTIR and laser Raman spectroscopy. It was found that without regard to the precipitation pH the first stage of ball-milling caused an increase of the crystallization temperature that resulted in the formation of pure t-ZrO_2. The second stage of ball-milling caused a decrease of the crystallization temperature resulting in the formation of m-ZrO_2. The ball-milling process also influenced the dependence of the crystallization enthalpy of zirconium hydroxide on the precipitation pH. In the case of zirconium hydroxide precipitated at pH 2.5, the ball-milling caused dehydration and an increase in its hygroscopy. The nature of these effects was discussed. The extension of FTIR spectra to the far infrared region made it possible to distinguish between t-ZrO_2 and m-ZrO_2 polymorphs by this technique. Also, the influence of laser power on the identification of ZrO_2 polymorphs by Raman spectroscopy was elaborated.

Keywords: Ball-milling; Crystallization temperature; DCS; FTIR; Laser Raman; Precipitation; Zirconium hydroxide polymorphs

1. Introduction

Monoclinic zirconia (m-ZrO_2) is a stable polymorph of ZrO_2 at standard temperature and pressure. At high temperature, the following ZrO_2 polymorph transfor-

* Corresponding author.

SSDI 0040-6031(95)02665-7

mations occur:

$$\text{monoclinic} \xrightarrow{1170\,^{\circ}\text{C}} \text{tetragonal} \xrightarrow{2370\,^{\circ}\text{C}} \text{cubic} \xrightarrow{2680\,^{\circ}\text{C}} \text{melt}$$

An orthorhombic modification of ZrO_2 can be obtained under high pressure conditions [1]. In the 1930s Clark and Reynolds [2] revealed a low temperature form of t-ZrO_2 as a thermal decomposition product of zirconium salts or zirconium hydroxide. The existence of metastable t-ZrO_2, which shows no difference to the high temperature form, is still the subject of discussion [3–10].

The influence of the precipitation chemistry of zirconium hydroxide on its thermal behavior was investigated by Davis [11] and Srinivasan et al. [12, 13], while Clearfield [14] discussed the mechanism of zirconium hydroxide precipitation.

The influence of mechanical treatment on the formation of m-ZrO_2 and t-ZrO_2 crystals was investigated in several works [15–17]. Štefanić et al. [18] examined the influence of the time of ball-milling on the thermal behavior of zirconium hydroxide obtained by rapid addition of base to a solution of the salt $ZrO(NO_3)_2 \cdot 2H_2O$ at pH 10.5. The authors established that the process of ball-milling increases the temperature of the crystallization, decreases crystallization enthalpy (ΔH_c) and causes dehydration of zirconium hydroxide (ΔH_d). On the basis of DSC and TGA results they concluded that crystallization of metastable t-ZrO_2 from zirconium hydroxide is not simple topotactic process.

X-ray powder diffraction (XRD) is the most important technique for identification of ZrO_2 polymorphs. The techniques of vibrational spectroscopy are also becoming important in the analysis of ZrO_2 polymorphs because of some advantages compared with XRD. For example, in some cases the techniques of vibrational spectroscopy can recognize a shorter range of crystallization in the samples which are amorphous to X-rays. Raman spectroscopy has often been used for the identification of ZrO_2 crystal phases [7, 19–25]. Sometimes, Raman spectroscopy can be more convenient than XRD for distinguishing between tetragonal and cubic ZrO_2 phases [19]. Infrared spectroscopy has been much less used, because only m-ZrO_2 could be easily recognized [25, 26]. From group theory it can be shown that t-ZrO_2 allows six Raman-active modes of vibration ($A_{1g} + 2B_{1g} + 3E_g$) and only three IR active ($A_{2u} + 2E_u$). From these three allowed vibrations only one broad band with transmittance minimum at $\sim 500\,cm^{-1}$ was observed by Phillipi and Mazdiyasni [25]; this could not be distinctly distinguished from the bands of cubic or amorphous zirconia. Recently, Štefanić et al. [8] observed two new IR-active bands, one typical of m-ZrO_2 at $177\,cm^{-1}$ and another, very strong and broad, with transmittance minimum at $\sim 180\,cm^{-1}$, typical of t-ZrO_2, which was also confirmed by Hirata et al. [27]. This new IR-active band made possible a distinct identification of t-ZrO_2 phase.

The present work brings new results obtained during the investigation of the influence of the pH of zirconium hydroxide precipitation and the mechanical treatment of this precipitate on its thermal behavior. Also, in the present work it is shown that FTIR spectroscopy can be used as an efficient technique for detection of t-ZrO_2 and m-ZrO_2 polymorphs.

2. Experimental

Amorphous zirconium hydroxide was precipitated at pH 10.5, 7.5 or 2.5 from a solution of $ZrOCl_2 \cdot 8H_2O$ salt by rapid addition of NH_4OH under vigorous stirring. The precipitates (samples $Z2_0$, $Z7_0$, and $Z10_0$) were washed eight times with doubly distilled water, separated from the aqueous phase by means of a Sorvall, RC2-B, ultra-speed centrifuge (operating range up to 20000 r.p.m.), dried at 70 °C for 24 h and subjected to ball-milling using a Fritsch (Pulverisette 5) planetary ball-mill with agate bowl and balls (99.9% SiO_2). The presence of SiO_2 impurities in ball-milled samples was not observed by FTIR and laser Raman spectroscopy, or by XRD [18]. The notation $Z10_x$, $Z7_x$, and $Z2_x$ given in Table 1, means precipitation at pH 10.5, 7.5 and 2.5, respectively, while the index x corresponds to the time of ball-milling. Ball-milled samples were heated inside a Perkin–Elmer differential scanning calorimeter (DSC), model 7, up to 600 °C with scanning rate of 20 °C per minute. During the measurements nitrogen was used as purge gas and circulating water as coolant. The instrument was coupled with a personal computer loaded with a program for processing the obtained

Table 1
The results obtained from DSC thermograms of ball-milled samples

Sample	Time of ball-milling/h	Dehydration		Crystallization		
		Enthalpy/ (kJ mol^{-1})	Maximum/°C	Enthalpy/ (kJ mol^{-1})	Maximum 1/ °C	Maximum 2/ °C
$Z2_0$	0	42	140	−13	469	–
$Z2_1$	1	90	127	−14	515	–
$Z2_3$	3	100	125	−16	514	–
$Z2_{10}$	10	110	125	−19	508	–
$Z2_{25}$	25	100	127	−14	506	–
$Z2_{40}$	40	70	117	−13	501	–
$Z7_0$	0	35	177	−20	468	–
$Z7_1$	1	29	179	−20	473	503
$Z7_3$	3	22	161	−20	473	507
$Z7_{10}$	10	17	147	−20	–	507
$Z7_{25}$	25	14	131	−20	–	514
$Z7_{40}$	40	17	144	−20	–	498
$Z7_{50}$	50	14	144	−19	–	493
$Z7_{60}$	60	13	140	−19	–	488
$Z10_0$	0	42	–	−21	457	–
$Z10_1$	1	33	138	−20	460	478
$Z10_3$	3	22	130	−19	465	489
$Z10_{10}$	10	11	138	−18	–	507
$Z10_{20}$	20	12	140	−14	–	525
$Z10_{30}$	30	18	144	−12	–	539
$Z10_{50}$	50	8	144	−11	–	533
$Z10_{60}$	60	5	180	−11	–	522

DSC curves. The molar values of the crystallization and dehydration enthalpy (ΔH_c and ΔH_d) were calculated using the mass difference before and after heating up to 1100 °C, and supposing that heated samples are pure ZrO_2. In all cases the ΔH_c and ΔH_d values represent enthalpy changes resulting from the complete process of dehydration and crystallization, obtained from the total area of the peak, irrespective of whether it contained one or two peak maxima.

Thermogravimetric (TG) analysis of the samples $Z7_0$ and $Z10_0$ was performed with a Mettler TG 50 coupled with a personal computer loaded with a program for processing the obtained TG curves. Measurements were performed up to 600 °C with scanning rate of 20 °C per minute. During the measurements argon was used as a purge gas.

Samples heated inside DSC up to 600 °C were analyzed by FTIR and laser Raman spectroscopy. FTIR spectra were recorded in the far infrared region with a Perkin–Elmer model 2000 spectrometer. The instrument was coupled with personal computer loaded with the IR Data Manager program. The samples were prepared for recording by gentle pressing onto the surface of polyethylene foil.

Laser Raman spectra recording was performed using a Dilor Z24 triple monocromator with 514.5 nm line of Coherent Innova-100 argon laser as excitation source. The laser power at sample was varied from 30 to 300 mW, because some samples showed susceptibility to the laser power used. The samples were prepared for recording by deposition into the recess of lead plate. This procedure ensured better heat transfer during the spectroscopic measurements.

3. Results and discussion

Fig. 1 shows the DSC curves of samples $Z10_0$, $Z10_1$, $Z10_3$, $Z10_{10}$, $Z10_{20}$, $Z10_{30}$, $Z10_{50}$, and $Z10_{60}$ while the corresponding thermochemical data are given in Table 1. Two exothermic peaks observed for heated samples $Z10_1$ and $Z10_3$ are very probably due to the heterogeneity of the grains resulting from ball-milling, as discussed in a previous paper [18].

The TG curve of sample $Z10_0$ showed continuous loss of mass between 50 and 300 °C; this corresponds to the temperature region of its endothermic peak in DSC curve. At higher temperatures, up to 600 °C, the mass of the sample stayed approximately the same. After differentiation of the TG curve two maxima appeared in the region of the mass losses, which indicates the uneven velocity of this process and explains the existence of two maxima in the endothermic peak of the DSC curve which resulted from the process of dehydration.

Fig. 2 shows FTIR spectra of heated samples $Z10_0$, $Z10_3$, $Z10_{20}$, $Z10_{50}$ and $Z10_{60}$. The spectra of heated samples $Z10_0$, $Z10_3$ and $Z10_{20}$, showed two broad bands at ~ 510 and $\sim 180\,cm^{-1}$ indicating the presence of t-ZrO_2 [8, 18]. The intensities of these bands increased with the time of ball-milling and reached a maximum for heated sample $Z10_{20}$. In heated samples $Z10_{50}$ and $Z10_{60}$ the bands typical of the t-ZrO_2 phase appeared together with bands at 579, 450 and $350\,cm^{-1}$ which indicated the appearance of m-ZrO_2 phase also; the amount of this increased with the time of ball-milling.

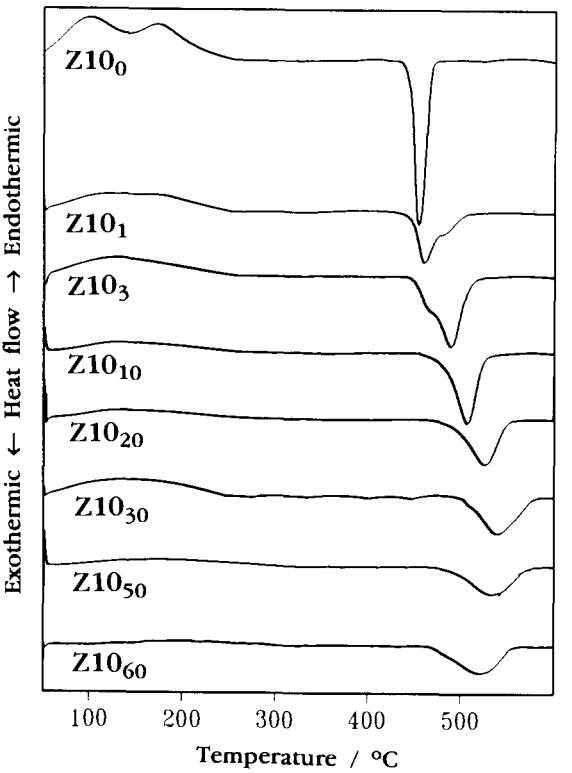

Fig. 1. DSC curves of the samples of zirconium hydroxide (series Z10) precipitated at pH 10.5 and mechanically treated for up to 60 h.

Fig. 3 shows laser Raman spectra of heated samples $Z10_0$, $Z10_{20}$ and $Z10_{50}$. The spectra of heated samples $Z10_0$ and $Z10_{20}$ showed Raman bands at 149, 265, and 465 cm^{-1} which are typical of t-ZrO_2 [7, 22–25]. The bands typical of m-ZrO_2 were not observed. These results are in agreement with the results of FTIR spectroscopy. Raman spectra of heated samples $Z10_0$ and $Z10_{50}$ were recorded with a laser power of 100 mW. In the case of heated sample $Z10_{20}$ the same laser power gave a Raman spectrum with very low intensity peaks, so the laser power was increased to 300 mW. High laser power used for Raman recording of this sample gave evidence of uneven distribution of the crystalline phase through the grain. The surface of the grain was probably coated with an amorphous layer that prevented laser beam from penetrating inside the grain and detecting the crystalline phase. The spectrum of heated sample $Z10_{50}$ showed bands at 374, 186, and 175 cm^{-1} typical of m-ZrO_2 [7, 8, 19–22] and at 470, 265, and 145 cm^{-1} typical of t-ZrO_2; this is in agreement with the corresponding FTIR spectrum.

Fig. 4 shows DSC curves of samples $Z7_0$, $Z7_1$, $Z7_3$, $Z7_{10}$, $Z7_{25}$, $Z7_{40}$, and $Z7_{60}$; the corresponding thermochemical data are given in Table 1. Samples $Z7_1$ and $Z7_3$ showed two exothermic peaks of crystallization. The intensity of the first peak at the lower temperature end was decreased by increasing the ball-milling time, whereas the second peak increased and shifted to higher temperature.

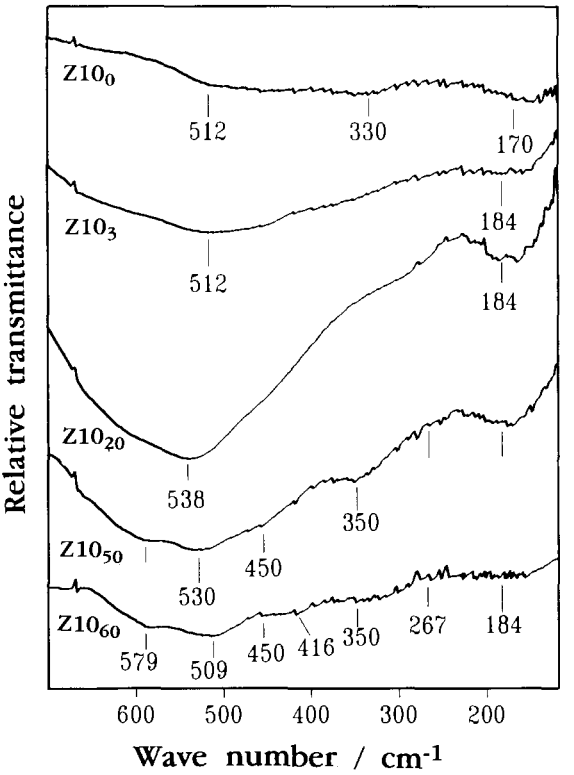

Fig. 2. FTIR spectra of heated samples $Z10_0$, $Z10_3$, $Z10_{20}$, $Z10_{50}$ and $Z10_{60}$.

The TG curve and the differential of the TG curve of sample $Z7_0$ showed, as in the case of sample $Z10_0$, that both maxima in the endothermic peak resulted from the process of dehydration.

Fig. 5 shows FTIR spectra of heated samples $Z7_0$, $Z7_1$, $Z7_{25}$, $Z7_{40}$, and $Z7_{50}$. The spectra of heated samples $Z7_1$ and $Z7_{25}$ as well as those (not shown) of heated samples $Z7_3$ and $Z7_{10}$ are typical of t-ZrO_2, and lack the bands characteristic of m-ZrO_2. The spectrum of heated sample $Z7_{40}$ showed bands typical of m-ZrO_2 [8, 25, 26], but the presence of a small portion of t-ZrO_2 phase could not be excluded. In the spectrum of heated sample $Z7_{50}$, as well as heated sample $Z7_0$, only bands typical of m-ZrO_2 were observed, but three bands at 572, 501, and 451 cm^{-1} of heated sample $Z7_0$ are shifted to higher wave numbers at 580, 534, and 457 cm^{-1} for the sample $Z7_{50}$.

Fig. 6 shows laser Raman spectra of heated samples $Z7_0$, $Z7_1$, $Z7_{25}$, and $Z7_{50}$. The spectrum of heated sample $Z7_0$ recorded with a laser power of 100 mW showed bands at 376, 332, 190, and 177 cm^{-1} typical of m-ZrO_2 [7, 8, 19–22]. Bands suggesting the presence of t-ZrO_2, were not observed. The spectrum of heated sample $Z7_1$, recorded with the same laser power, showed bands at 267 and 145 cm^{-1} typical of t-ZrO_2 phase.

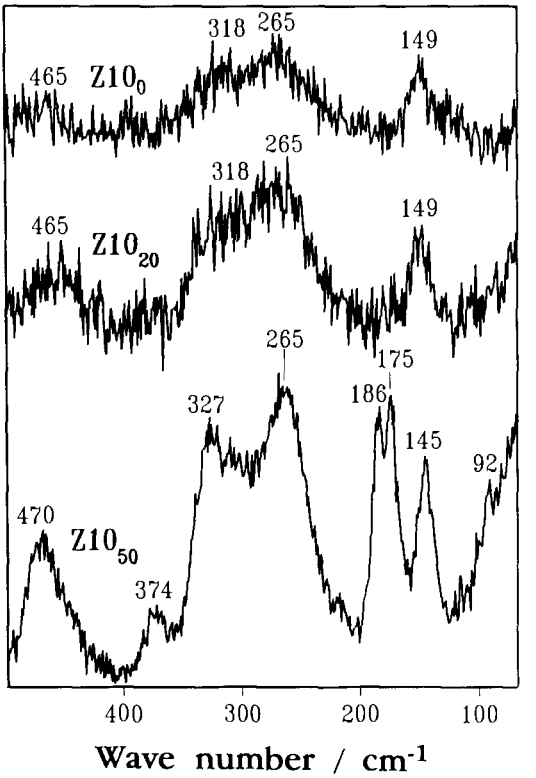

Fig. 3. Laser Raman spectra of heated samples $Z10_0$, $Z10_{20}$, and $Z10_{50}$.

The spectrum of heated sample $Z7_{25}$, recorded with a laser power of 30 mW, showed bands of pure t-ZrO_2 phase without the features of m-ZrO_2. Weak laser power was used because a stronger laser beam caused phase transformation in this sample. The spectrum of heated sample $Z7_{50}$, recorded with a laser power of 50 mW, showed only bands typical of m-ZrO_2; this is in agreement with results obtained by FTIR.

Fig. 7 shows DSC curves of samples $Z2_0$, $Z2_1$, $Z2_3$, $Z2_{10}$, $Z2_{25}$ and $Z2_{40}$; the corresponding thermochemical data are given in Table 1. The analysis of these curves indicated that the endothermic peak of dehydration was increased by increasing the time of ball-milling, from $\Delta H_d = 42\,kJ\,mol^{-1}$ for sample $Z2_0$ to the maximum value of $\Delta H_d = 110\,kJ\,mol^{-1}$ for sample $Z2_{10}$. With a prolonged ball-milling time a decrease in peak intensity ($\Delta H_d = 70\,kJ\,mol^{-1}$ for sample $Z2_{40}$) was observed. The loss of mass during heating of the samples up to 1100 °C supported this observation. Samples $Z2_0$, $Z2_{10}$, $Z2_{25}$, and $Z2_{40}$ lost 37, 54, 51, and 44%, respectively, of their initial mass. On the basis of these results it can be concluded that ball-milling caused two opposite phenomena–dehydration of the sample with an increase in hygroscopy. The temperature of the crystallization was increased by increasing the time of ball-milling, reaching a maximum after ~ 1 h. With a prolonged ball-milling time the temperature of the

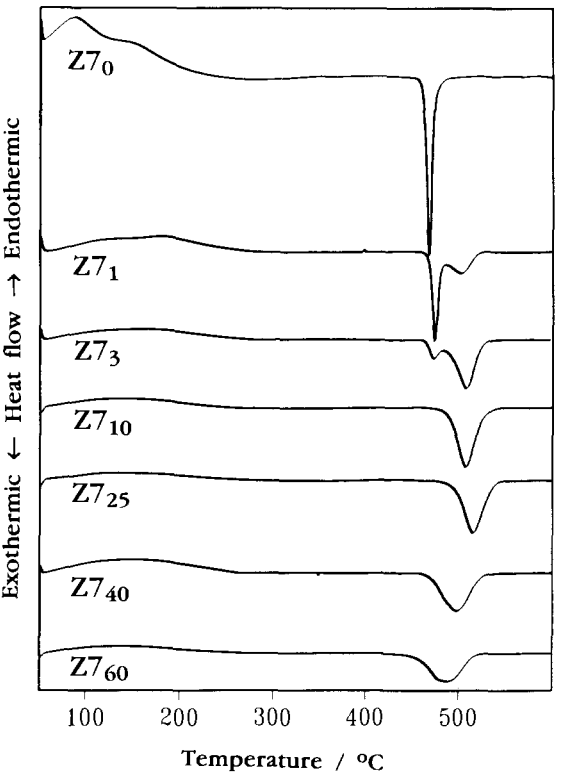

Fig. 4. DSC curves of the samples of zirconium hydroxide (series Z7) precipitated at pH 7.5 and mechanically treated for up to 60 h.

crystallization was decreased. The intensity of the crystallization peak of sample $Z2_0$, which was not affected by ball-milling, was $-13\,kJ\,mol^{-1}$, which was much smaller than the intensity for samples which were precipitated at pH 7.5 and 10.5 and not ball-mill. The ball-milling of sample $Z2_0$ caused an increase of peak intensity to a maximum value of $\Delta H_c = -19.0\,kJ\,mol^{-1}$ for sample $Z2_{10}$, and a prolonged ball-milling time caused a decrease of peak intensity, $\Delta H_c = -13\,kJ\,mol^{-1}$ for sample $Z2_{40}$.

Fig. 8 shows FTIR spectra of heated samples $Z2_0$, $Z2_{0.5}$, $Z2_1$, $Z2_3$, $Z2_{25}$, and $Z2_{40}$. The spectrum of heated sample $Z2_0$ showed bands characteristic of t-ZrO_2 and m-ZrO_2 with the t-ZrO_2 phase predominant. The spectrum of heated sample $Z2_{0.5}$ indicated a decrease in the m-ZrO_2 content, while the spectrum of heated sample $Z2_1$ indicated pure t-ZrO_2 without the presence of m-ZrO_2 bands. The spectrum of heated sample $Z2_3$ indicated the presence of t-ZrO_2 phase; a small amount of m-ZrO_2 could not, however, be excluded due to the shoulders at 587, 453, and $350\,cm^{-1}$. The spectrum of heated sample $Z2_{25}$ indicated the appearance of m-ZrO_2 phase and a corresponding decrease of bands typical of t-ZrO_2. In the spectrum of heated sample $Z2_{40}$ only bands typical of m-ZrO_2 were observed.

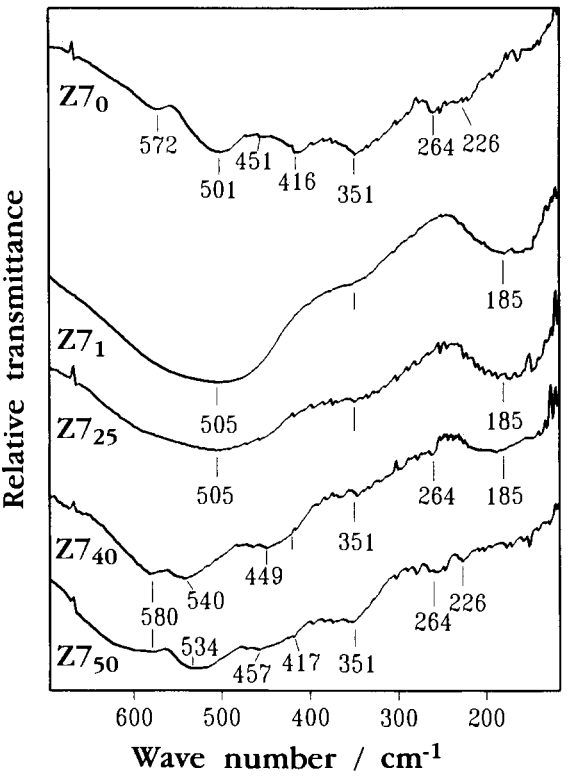

Fig. 5. FTIR spectra of heated samples $Z7_0$, $Z7_1$, $Z7_{25}$, $Z7_{40}$, and $Z7_{50}$.

Fig. 9 shows the laser Raman spectra of heated samples $Z2_0$, $Z2_1$, $Z2_{25}$, and $Z2_{40}$. The spectrum of heated sample $Z2_0$, recorded with a laser power of 75 mW, showed bands characteristic of the t-ZrO_2 and m-ZrO_2 phases with more intense t-ZrO_2 bands, as in the case of the FTIR spectrum. In the spectrum of heated sample $Z2_1$, recorded with a laser power of 100 mW, only bands characteristic of the t-ZrO_2 phase were observed. These results indicated that a short ball-milling time has an influence on the structure of zirconium hydroxide in such a way as to produce t-ZrO_2 phase after heating, similar, as to heated samples of zirconium hydroxide precipitated at pH 7.5. The spectra of heated samples $Z2_{25}$ and $Z2_{40}$ contained bands typical of both t-ZrO_2 and m-ZrO_2. The proportion of m-ZrO_2 phase increased with increasing ball-milling time.

Fig. 10 illustrates the dependence of the crystallization temperature of zirconium hydroxide, precipitated at three different pH values, on the time of ball-milling. The points in this figure representing the values of the crystallization temperature of samples $Z7_1$, $Z7_3$, $Z10_1$ and $Z10_3$ were approximated, because these samples showed two peak maxima, probably, because of heterogeneity of the grains. The curves obtained indicated that in all cases an early stage of ball-milling caused an increase of

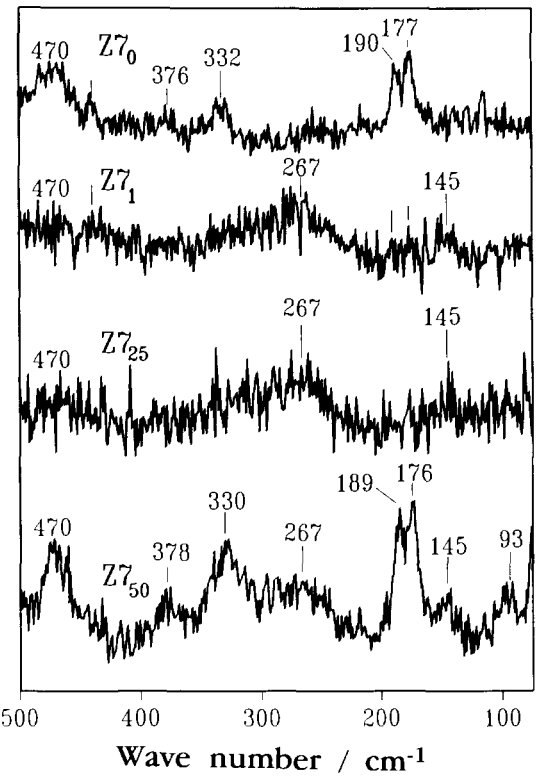

Fig. 6. Laser Raman spectra of heated samples $Z7_0$, $Z7_1$, $Z7_{25}$, and $Z7_{50}$.

the crystallization temperature, and also that the extent of this effect depended on the precipitation pH. In the first hour of ball-milling the crystallization temperature increased by $\sim 5\,^{\circ}C$ for the sample precipitated at pH 10.5, $\sim 15\,^{\circ}C$ for the sample precipitated at pH 7.5, and $\sim 50\,^{\circ}C$ for the sample precipitated at pH 2.5 thus suggesting that higher precipitation pH produced tougher grains of zirconium hydroxide, more resistant to the disordering process caused by ball-milling. With prolonged ball-milling time the maximum values of the crystallization temperature were reached, and then with further ball-milling the crystallization temperature decreased. The decrease of the crystallization temperature could be attributed to the effect of ball-milling that became observable after prolonged ball-milling time, i.e., when the disordering of zirconium hydroxide structure reached the maximum. The ball-milling time needed to obtain the maximum value of the crystallization temperature increased with increasing pH of zirconium hydroxide precipitation, from 1 h at pH 2.5 and 20 h at pH 7.5 to 35 h at pH 10.5. It is interesting to note that at the point corresponding to 10 h of ball-milling the crystallization temperature was independent of the precipitation pH.

Fig. 11 shows the dependence of ΔH_c of zirconium hydroxide, precipitated at three different pH values, on the time of ball-milling. The curve corresponding to the samples

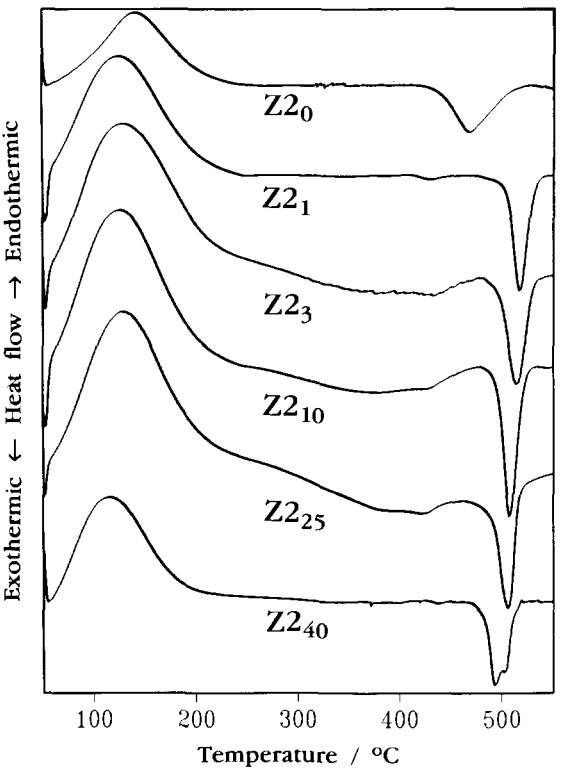

Fig. 7. DSC curves of the samples of zirconium hydroxide (series Z2) precipitated at pH 2.5 and mechanically treated for up to 40 h.

of zirconium hydroxide precipitated at pH 2.5 showed an increase of ΔH_c with increasing ball-milling time up to 10 h. With prolonged ball-milling ΔH_c decreased. The ΔH_c of zirconium hydroxide samples precipitated at pH 7.5 were shown to be independent of the ball-milling time. The curve corresponding to the samples of zirconium hydroxide precipitated at pH 10.5 showed a decrease of ΔH_c with increasing ball-milling time until, after prolonged ball-milling, saturation was reached. The rate by which ΔH_c decreased was smaller than that measured for zirconium hydroxide precipitated at the same pH from the solution of the $ZrO(NO_3)_2 \cdot 2H_2O$ salt [18].

On the basis of the results presented it could be concluded that, without regard to the precipitation pH, a short ball-milling time has an influence on the structure of zirconium hydroxide in a way which increases the temperature of its crystallization, resulting in the formation of t-ZrO_2, whereas long ball-milling times reduce the crystallization temperature resulting in the formation of m-ZrO_2. These results suggested the need to reinvestigate the Clearfield theory [14]. Clearfield concluded that tetrameric units, $[Zr(OH)_2 \cdot 4H_2O]_4^{8+}$, present in solutions of zirconium salts, underwent polymerization during hydroxide precipitation. If the precipitation process was fast only a small number of tetrameric units were linked together, which resulted in the

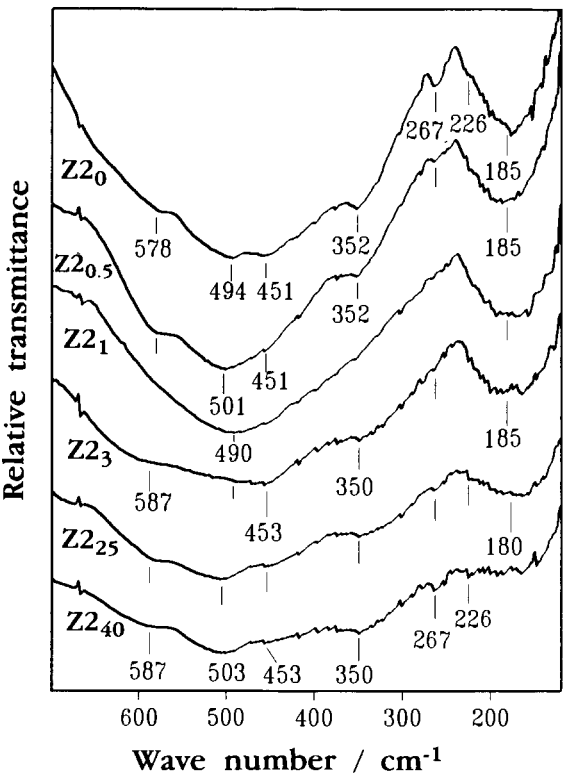

Fig. 8. FTIR spectra of heated samples $Z2_0$, $Z2_{0.5}$, $Z2_1$, $Z2_3$, $Z2_{25}$, and $Z2_{40}$.

formation of amorphous gel which, on heating, was converted to m-ZrO_2. Slow addition of base during the precipitation process led to polymerization and formation of two-dimensional sheets that linked together to form a fluorite structure which, after heating, produced t-ZrO_2. The interpretation of our results in light of this theory [14] led to the conclusion that ball-milling of amorphous gel (obtained by fast precipitation) caused an ordering and linking of small randomly oriented structural units which resulted in the formation of the structure similar to that obtained by slow precipitation of zirconium hydroxide. However, it is our opinion that ball-milling has no ability to cause such structural organization, so we do not prefer the Clearfield theory [14] to explain thermal behavior of ball-milled zirconium hydroxide. A possible explanation of the formation of t-ZrO_2 after heating of ball-milled zirconium hydroxide is suggested in our earlier work [18]. We suggested that ball-milling occasionally transfers enough energy to a small part of grain to cause formation of t-ZrO_2 crystals in a very small domain. These tiny t-ZrO_2 crystals generated in ball-milled zirconium hydroxide can govern the process of crystallization to t-ZrO_2 crystal phase. On the other hand, the formation of m-ZrO_2 phase, after heating of zirconium hydroxide ball-milled for a long-time, indicated a ball-milling process of a more complex nature.

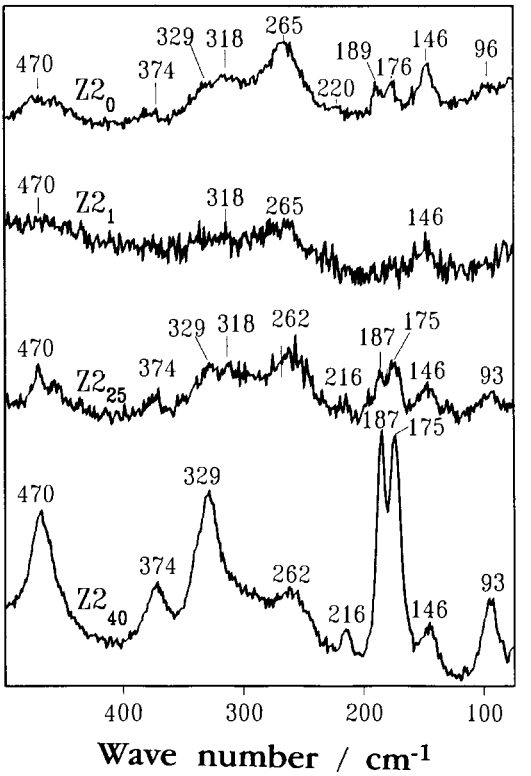

Fig. 9. Laser Raman spectra of heated samples $Z2_0$, $Z2_1$, $Z2_{25}$, and $Z2_{40}$.

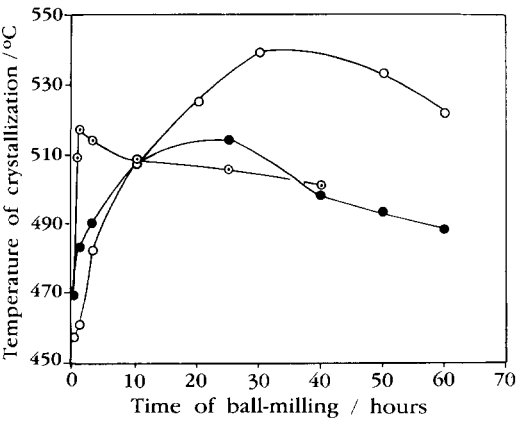

Fig. 10. The temperature of crystallization of zirconium hydroxide as a function of the ball-milling time: ○ = Z10, ● = Z7, ⊙ = Z2.

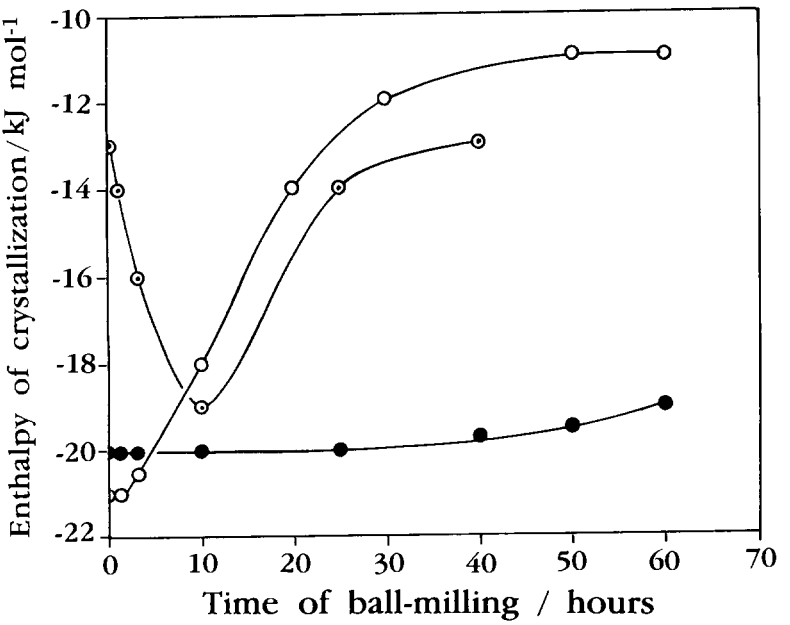

Fig. 11. The enthalpy of crystallization of zirconium hydroxide as a function of the ball-milling time: ○ = Z10, ● = Z7, ⊙ = Z2.

References

[1] L. Lenz and A.H. Heuer, J. Am. Ceram. Soc., 65 (1982) C-192.
[2] I. Clark and D.H. Reynolds, Ind. Eng. Chem., 29 (1937) 711.
[3] R. Cypres, R. Wollast and J. Raucq, Ber. Dtsch. Keram. Ges., 40 (1963) 527.
[4] R.C. Garvie, J. Phys. Chem., 69 (1965) 1238.
[5] T. Mitsuhasi, M. Ichihara and U. Tatsuke, J. Am. Ceram. Soc., 57 (1974) 97.
[6] J. Livage, K. Doi and C. Mazieres, J. Am. Ceram. Soc., 51 (1968) 349.
[7] G. Keramidas and W.B. White, J. Am. Ceram. Soc., 57 (1974) 22.
[8] G. Štefanić, S. Musić, S. Popović and K. Furić, Croat. Chem. Acta, in press
[9] J. Torralvo, M.A. Alario and J. Soria, J. Catal., 86 (1984) 473.
[10] I. Osendi, I.S. Moya, C.I. Serna and I. Soria, J. Am. Ceram. Soc., 68 (1985) 135.
[11] B.H. Davis, J. Am. Ceram. Soc., 67 (1984) C-168.
[12] R. Srinivasan, R.J. DeAngelis and B.H. Davis, J. Mater. Res., 1 (1986) 583.
[13] R. Srinivasan, M.B. Harris, S.F. Simpson, R.J. DeAngelis and B.H. Davis, J. Mater. Res., 3 (1988) 787.
[14] A. Clearfield, J. Mater. Res., 5 (1990) 161.
[15] E. Bailey, D. Lewis, Z.M. Librant and L.J. Porter, Trans. Br. Ceram. Soc., 71 (1972) 25.
[16] A.N. Scian, E.F. Aglietti, M.C. Caracohe, P.C. Rivas, A.F. Pasquevich and A.R.L. Garcia, J. Am. Ceram. Soc., 77 (1994) 1525.
[17] Y. Murase and E. Kato, J. Am. Ceram. Soc., 62 (1979) 527.
[18] G. Štefanić, S. Musić and S. Popović, Thermochim. Acta, in press.
[19] R. Srinivasan, S.F. Simpson, J. M. Harris and B.H. Davis, J. Mater. Sci. Lett., 10 (1991) 352.
[20] D.M. Lui, C.H. Perry and R.P. Ingel, J. Appl. Phys., 64 (1988) 1415.
[21] H. Arashi and M. Ishigame, Phys. Status Solidi, 71 (1982) 313.
[22] C.H. Perry, F. Lu, D.W. Liu and B. Alzyab, J. Raman Spectrosc., 21 (1990) 577.

[23] D.J. Kim, H. Jung and I.S. Yang, J. Am. Ceram. Soc., 76 (1993) 2106.
[24] M. Yashima, H. Arashi, M. Kakihana and M. Yoshimura, J. Am. Ceram. Soc., 77 (1994) 1067.
[25] C.M. Phillippi and K.S. Mazdiyasni, J. Am. Ceram. Soc., 54 (1971) 254.
[26] N.T. Mcdevitt and W.L. Baun, J. Am. Ceram. Soc., 47 (1964) 622.
[27] T. Hirata, E. Asari and M. Kitajima, J. Solid State. Chem., 110 (1994) 201.